Jin Wang
Department of Mechanical Engineering,
Boston University,
Boston, MA 02215

Thao D. Nguyen
Department of Mechanical Engineering,
The Johns Hopkins University,
Baltimore, MD 21218

Harold S. Park[1]
Department of Mechanical Engineering,
Boston University,
Boston, MA 02215
e-mail: parkhs@bu.edu

Electrostatically Driven Creep in Viscoelastic Dielectric Elastomers

We utilize a nonlinear, dynamic finite element model coupled with a finite deformation viscoelastic constitutive law to study the inhomogeneous deformation and instabilities resulting from the application of a constant voltage to dielectric elastomers. The constant voltage loading is used to study electrostatically driven creep and the resulting electromechanical instabilities for two different cases that have all been experimentally observed, i.e., electromechanical snap-through instability and bursting drops in a dielectric elastomer. We find that in general, increasing the viscoelastic relaxation time leads to an increase in time needed to nucleate the electromechanical instability. However, we find for these two cases that the time needed to nucleate the instability scales with the relaxation time. [DOI: 10.1115/1.4025999]

1 Introduction

Dielectric elastomers (DEs) are a class of soft, active materials that have attracted significant attention in recent years [1–6]. They have been found to provide excellent overall performance in actuation-based applications, including high specific elastic energy density, good efficiency, and high speed of response (on the order of milliseconds). Furthermore, DEs are typically lightweight, flexible, and inexpensive materials which makes them ideal candidates for high performance, low cost applications where fabrication of the DEs into a wide range of shapes and structures can easily be realized [7]. While DEs have been found to exhibit good performance with respect to a variety of actuation-relevant properties, the key source of the technological excitement surrounding DEs stems from the fact that, if sandwiched between two compliant electrodes that apply voltage to the elastomer, the DE can exhibit both significant thinning and in-plane expansion. This unique large deformation-based actuation capability has led to many potential applications for DEs, including medical devices, artificial muscles, and the potential to harvest energy from sources as diverse as human muscle motion and ocean waves [1,2,5].

However, it has been understood for some time that viscoelastic effects play a crucial role in determining the large-deformation response of the DEs [8]. Viscoelastic effects are important because the dominant failure mode of DEs is strongly dependent on both the stretch rate and the amount of prestrain [9]. This is because at higher stretch rates and frequencies, viscoelastic effects stiffen the material, which limits the force generation, efficiency, and actuation speed, while simultaneously introducing the deleterious effects of creep, hysteresis, and stress relaxation. Correspondingly, there has recently been an increasing effort in the research community to study, both experimentally and theoretically, viscoelastic effects on the behavior of DEs [3,8–18].

A key issue that has not been studied in detail is the creep response of DEs to a constant electrostatic (i.e., voltage) load, particularly in the context of electromechanical instabilities that can result in DEs. For example, a recent analytical study on electrostatically driven creep in viscoelastic DEs was performed by Wang et al. [14]. However, due to the simplicity of the analytical model, the authors did not consider electromechanical instabilities for interesting and important DE failure modes such as electromechanical snap-through [9,19] and cracklike initiation and propagation [20].

The objective of this paper is to utilize a recently developed nonlinear, finite deformation viscoelastic finite element (FE) model of DEs [16] to study the creep response of DEs under constant electrostatic (voltage) loading. We do this in the context of focusing on the effects of viscoelasticity on the characteristics of two electromechanical instabilities that have been observed experimentally to cause failure in DEs: snap-through instability [9,21], and cracklike propagation emerging from a bursting drop in a DE [20].

2 Field Theory and Finite Element Model

The electromechanical field theory [22], and the resulting FE equations, have previously been discussed in detail in previous publications [16,23,24], so we give only a brief overview here.

The numerical results we present in this work are based upon a FE discretization of the electromechanical field theory recently proposed by Suo et al. [22], and recently reviewed by Suo [25]. In this field theory at mechanical equilibrium, the nominal stress S_{iJ} satisfies the following weak form of the momentum balance equation:

$$\int_V S_{iJ}\frac{\partial \xi_i}{\partial X_J}dV = \int_V \left(B_i - \rho\frac{\partial^2 x_i}{\partial t^2}\right)\xi_i\, dV + \int_A T_i\xi_i\, dA \tag{1}$$

where ξ_i is an arbitrary vector test function, B_i is the body force per unit reference volume V, ρ is the mass density of the material, and T_i is the force per unit area that is applied on the surface A in the reference configuration.

For the electrostatic problem, the nominal electric displacement $\tilde{D}_I$ satisfies the following weak form of the governing equation:

$$-\int_V \tilde{D}_I\frac{\partial \eta}{\partial X_I}dV = \int_V q\eta\, dV + \int_A \omega\eta\, dA \tag{2}$$

where η is an arbitrary scalar test function, q is the volumetric charge density, and ω is the surface charge density, both with respect to the reference configuration. It can be seen that the strong form of the electrostatic weak form in (2) corresponds to Gauss's law.

As the governing field equations in (1) and (2) are decoupled, the electromechanical coupling occurs through the material laws. Due to the fact that the DE is a rubberlike polymer, phenomenological free energy expressions are typically used to model the deformation of the polymer chains. In the present work, we utilize the form [26,27]

$$W_{\text{eq}}(\mathbf{C},\tilde{\mathbf{E}}) = \mu_{\text{eq}}W_0 - \frac{1}{2}K(\ln J)^2 - 2\mu_{\text{eq}}W_0(3)\ln J - \frac{\varepsilon}{2}JC_{IJ}^{-1}\tilde{E}_I\tilde{E}_J \tag{3}$$

[1]Corresponding author.

Contributed by the Applied Mechanics Division of ASME for publication in the Journal of Applied Mechanics. Manuscript received October 20, 2013; final manuscript received November 4, 2013; accepted manuscript posted November 11, 2013; published online December 10, 2013. Editor: Yonggang Huang.

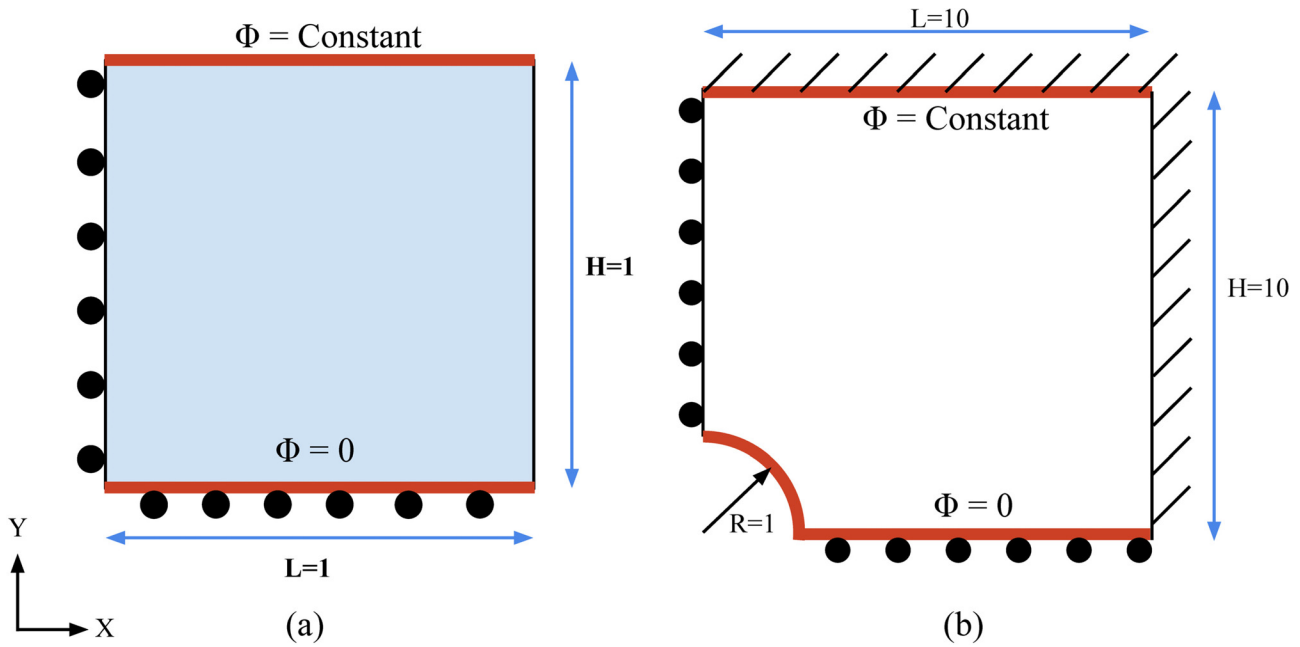

Fig. 1 Schematic of the two problems considered, with mechanical and electrostatic boundary conditions shown. (*a*) Single finite element for electromechanical snap-through problem. (*b*) Quarter symmetry model for bursting drop in a DE. Note that all schematics are shown in two dimensions as all *z* displacements are set to zero in this work to mimic a plane strain problem.

where W_0 is the mechanical free energy density in the absence of an electric field, ε is the permittivity, $\tilde{\mathbf{E}}$ is the nominal electric field, $J = \det(\mathbf{F})$, where $\mathbf{F}$ is the continuum deformation gradient, C_{IJ}^{-1} are the components of the inverse of the right Cauchy–Green tensor $\mathbf{C}$, K is the bulk modulus, and μ_{eq} is the equilibrium shear modulus. We distinguish the free energy W_{eq} in (3) as the equilibrium free energy as the nonequilibrium terms that appear later capture the viscoelastic effects.

We model the mechanical behavior of the DE using the Arruda–Boyce rubber hyperelastic function [28]. The mechanical free energy W_0 in (3) is approximated by the following truncated series expansion:

$$\frac{W_0(I_1)}{\mu} = \frac{1}{2}(I_1 - 3) + \frac{1}{20N}(I_1^2 - 9) + \frac{11}{1050N^2}(I_1^3 - 27) + \frac{19}{7000N^3}(I_1^4 - 81) + \frac{519}{673750N^4}(I_1^5 - 243) \tag{4}$$

where N is a measure of the cross-link density, I_1 is the trace of $\mathbf{C}$, and where the Arruda–Boyce model reduces to a neo-Hookean model if $N \to \infty$. We emphasize that previous experimental studies of Wissler and Mazza [29] have validated the Arruda–Boyce model as being highly accurate for modeling the large deformation of DEs.

The FE equations that result from the discretization of Eqs. (1) and (2), accounting for finite nonlinear viscoelasticity using the approach of Reese and Govindjee [30], were derived by Park and Nguyen [16]. The resulting coupled electromechanical FE equations are

$$\begin{pmatrix} \Delta\mathbf{a} \\ \Delta\Phi \end{pmatrix} = -\begin{pmatrix} \mathbf{M} + \beta\Delta t^2(\mathbf{K}^{\text{eq}}_{mm+q1p0} + \mathbf{K}^{\text{neq}}_{mm}) & \mathbf{K}_{me} \\ \beta\Delta t^2\mathbf{K}_{em} & \mathbf{K}_{ee} \end{pmatrix}^{-1} \begin{pmatrix} \mathbf{R}_{\text{mech}} \\ \mathbf{R}_{\text{elec}} \end{pmatrix} \tag{5}$$

where $\mathbf{a}$ is the acceleration, Φ is the voltage, $\mathbf{M}$ is the lumped FE mass matrix, $\beta = 0.25$ is a constant needed for the classical Newmark time integration algorithm [31], Δt is the time step, $\mathbf{K}^{\text{eq}}_{mm+q1p0}$ is the equilibrium mechanical stiffness matrix, $\mathbf{K}^{\text{neq}}_{mm}$ is the viscoelastic (nonequilibrium) contribution to mechanical stiffness that is calculated following the finite viscoelasticity formulation of Reese and Govindjee [30], $\mathbf{K}_{em} = \mathbf{K}_{me}$ is the electromechanical stiffness coupling, and $\mathbf{K}_{ee}$ is the purely electrostatic stiffness.

Table 1 Values of the material parameters needed to evaluate the equilibrium free energy W_{eq} in Eq. (3), the Arruda–Boyce hyperelastic function in Eq. (4), and the nonequilibrium viscoelastic formulation

Material parameter	Value
N	5.0
μ_{eq}	1.0 Pa
ε	1.0 F/m
K	10,000.0 Pa
μ_{neq}	1.0 Pa

Finally, the mechanical stiffness matrix $\mathbf{K}^{\text{eq}}_{mm+q1p0}$ in (5) can be written

$$\mathbf{K}^{\text{eq}}_{mm+q1p0} = \mathbf{K}_{\text{geo}} + \mathbf{K}_{\text{mat}} + \mathbf{K}_p \tag{6}$$

where $\mathbf{K}_{\text{geo}}$ and $\mathbf{K}_{\text{mat}}$ are the standard geometric and material contributions to the stiffness matrix, and where $\mathbf{K}_p$ is a new contribution to the stiffness matrix that comes from the Q1P0 formulation of Simo et al. [32], and that is required to alleviate the material incompressibility and prevent the FE formulation from exhibiting volumetric locking, or an overly, artificially stiff mechanical response. Details regarding the explicit forms of all stiffness contributions in Eq. (5) can be found in [23,24] and [16].

To summarize, the FE formulation we use in the present work: (1) Accounts for finite, nonlinear viscoelasticity, which is important for accurate predictions of creep [30,33]; and (2) alleviates volumetric locking which occurs due to the incompressible nature of DEs using the seminal Q1P0 formulation of [32]. Having established the governing equations and FE model, we now proceed to applying them to problems involving electrostatically driven creep in DEs.

3 Numerical Results

We considered two different problems, as illustrated in Fig. 1. The specific problems are the electromechanical snap-through instability [9,21,23] in Fig. 1(*a*), and a bursting drop in a solid

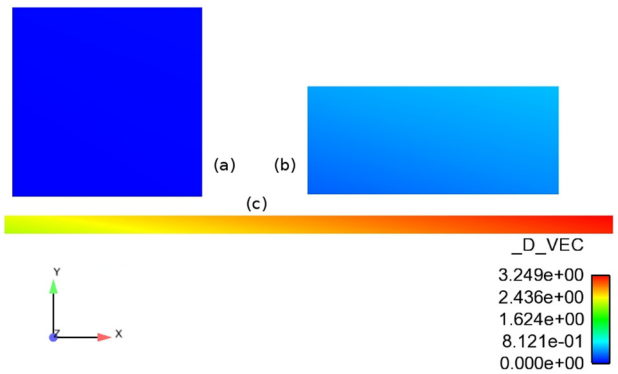

Fig. 2 Illustration of different stages of electromechanical snap-through instability. (*a*) Undeformed configuration. (*b*) Prior to snap-through instability. (*c*) Final configuration after snap-through instability has occurred. _D_VEC is the magnitude of the displacement vector.

[16,20] as shown in Fig. 1(*b*). These problems were chosen as a different type of electromechanical instability (snap-through, cracklike propagation) has been observed experimentally for each case.

In each case, a constant voltage Φ was applied starting at time $t = 0$ to simulate an electrostatically driven creep process, and the DE was then allowed to relax to equilibrium. We note that the critical values for the voltage Φ needed to induce electromechanical instabilities for all both problems have previously been established [20,21], and so constant voltages both smaller and larger than the critical voltage were applied in both cases.

All FE simulations considered the generalized three-dimensional geometry, and were conducted using eight-node hexahedral elements using the open source simulation code, Tahoe [34]. For the bursting drop problem in Fig. 1(*b*), the out of plane (z) displacement was set to zero to mimic a plane strain condition.

A key parameter that was varied for each problem below is the viscoelastic relaxation time $\tau_r = \eta/\mu_{\text{neq}}$, where η is the shear viscosity, and μ_{neq} is the nonequilibrium shear modulus. In all cases

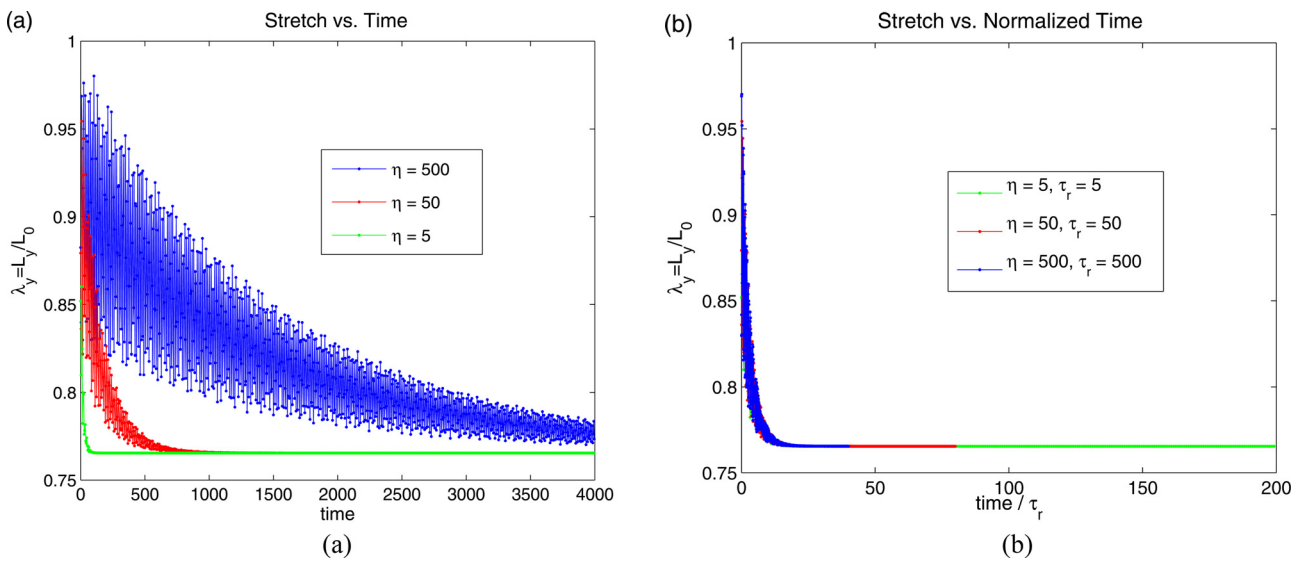

Fig. 3 Time evolution of thickness-direction stretch λ_y for an applied normalized voltage of $\Phi = 0.7$, or smaller than the critical voltage needed to cause the snap-through instability, for different viscosities η. (*a*) Not time normalized. (*b*) Normalized by the viscoelastic relaxation time τ_r.

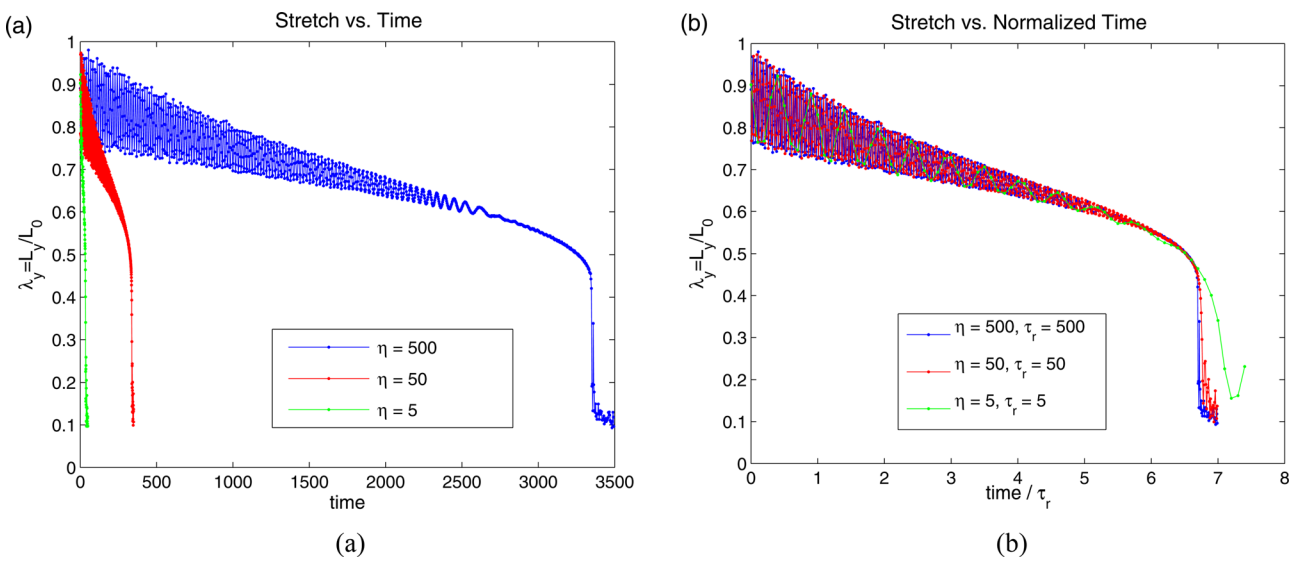

Fig. 4 Time evolution of thickness-direction stretch λ_y for a constant normalized voltage of $\Phi = 0.8$, or above the critical voltage needed to cause snap-through instability, for different viscosities η. (*a*) Not time normalized. (*b*) Normalized by the viscoelastic relaxation time τ_r.

$\mu_{neq} = 1$, and the viscosity η was varied, except for the bursting drop problem, over three orders of magnitude to create a corresponding three order of magnitude range of viscoelastic relaxation times τ_r. The material properties and parameters we used for the FE simulations to evaluate the free energy in Eq. (3) and the Arruda–Boyce model in Eq. (4), as well as the nonequilibrium viscoelastic parameters, are provided in Table 1.

3.1 Electromechanical Snap-Through Instability. The first example we consider is that shown in Fig. 1(*a*), which is used to study viscoelastic effects on the well-known electromechanical snap-through instability [9,21,23]. In this problem, it is known that above a critical normalized voltage of about $\Phi = 0.75$ [23], the electrostatic Maxwell stress becomes larger than the mechanical stress in the DE, causing a rapid decrease in thickness of the DE of nearly 90% and a substantial increase in the cross sectional area of the DE, as illustrated in Fig. 2. For this problem, a single eight-node hexahedral element was used subject to the electromechanical boundary conditions shown in Fig. 1(*a*).

We plot in Fig. 3 the vertical stretch $\lambda_y = L_y/L_0$ as a function of time as the shear viscosity η is varied between 5 and 500. Specifically, the cases shown in Fig. 3 demonstrate the behavior of the DE if the applied voltage of $\Phi = 0.7$ is smaller than the critical voltage $\Phi_{crit} = 0.75$. In Fig. 3(*a*) it can be seen that as η is increased, the DE takes a longer amount of time to creep to the same stretch λ_y, though all asymptotically reach the equilibrium value of $\lambda_y = 0.77$. However, Fig. 3(*b*) shows that if the time is normalized by the viscoelastic relaxation time, then all curves collapse to the same stretch value λ_y at the same normalized time.

Figure 4 shows the results for when the applied voltage of $\Phi = 0.8$ is larger than the critical voltage for instability of $\Phi_{crit} = 0.75$. As can be seen in Fig. 4(*a*), as η increases, the time needed for the snap-through instability to occur increases substantially, where the occurrence of the snap-through instability can be observed through the nearly instantaneous decrease in stretch λ_y near a critical stretch of about $\lambda_y = 0.5$ to a final value of about $\lambda_y = 0.1$, or a decrease in thickness of nearly 90%. This applied voltage of $\Phi = 0.8$ is larger than the critical voltage to induce creep for the equilibrium ($\mu = \mu_{eq}$) case, which is why the deformation in Fig. 4 has an initial creep stage followed by the snap-through instability.

However, Fig. 4(*b*) demonstrates that if the time is normalized by the viscoelastic relaxation time τ_r, that all curves collapse, with the onset of the snap-through instability occurring at the same normalized time of about $t/\tau_r = 6.65$. This demonstrates that for the snap-through instability problem, aside from increasing the critical voltage needed to induce the snap-through instability [16], the major effect of viscoelasticity is to proportionately increase the time needed for the snap-through instability to occur in direct proportion to the viscoelastic relaxation time τ_r.

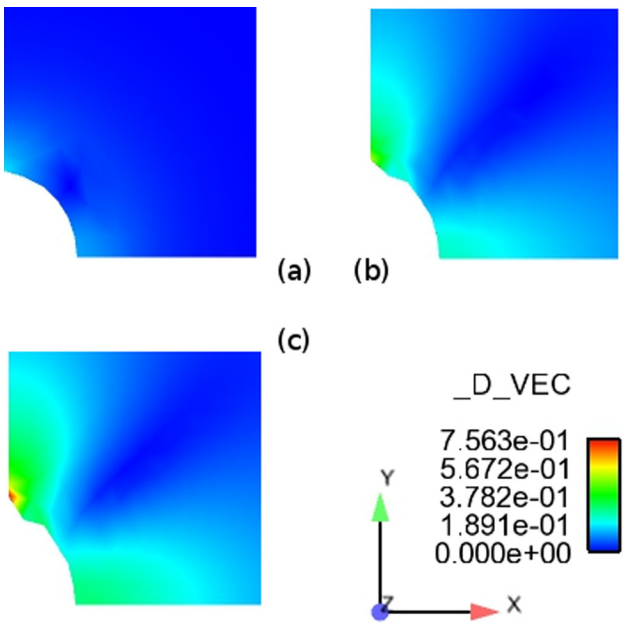

Fig. 5 Illustration of electrostatically driven crack initiation and propagation in a DE containing a conductive drop. Note the formation and propagation of a crack from the top of the hole. _D_VEC is the magnitude of the displacement vector.

3.2 Bursting Drops in a Confined Dielectric Elastomer. Our second and final example considers a numerical study of electrostatically driven creep, or specifically cracklike initiation and propagation from a bursting drop in a constrained DE, similar to the recent experiment of Wang et al. [20]. In that experiment, a

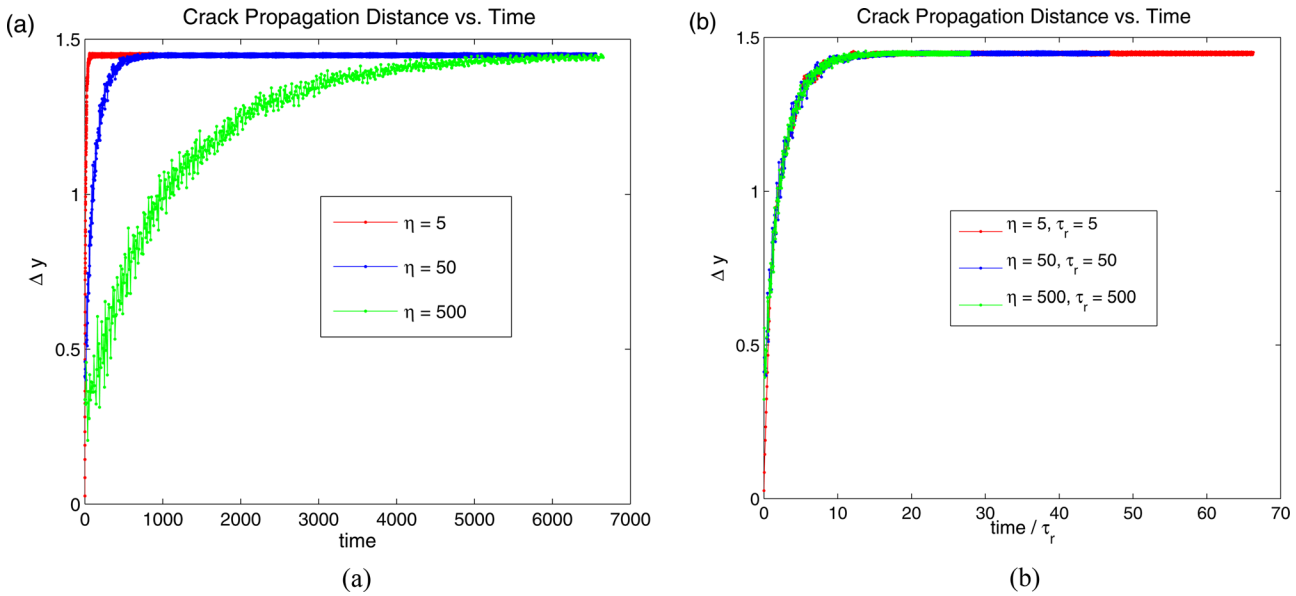

Fig. 6 (*a*) Crack propagation distance Δy as a function of time for different shear viscosities η. (*b*) Crack propagation distance Δy as a function of normalized time.

constrained DE film was created with a small hole containing a conductive liquid, i.e., a salt solution. Upon application of a voltage, the hole was found to change shape from a sphere to an elongated ellipsoid, followed by bursting of the drop in the hole via crack nucleation and propagation from the top of the hole, where this process is illustrated in Fig. 5. This problem was recently computationally studied by Park and Nguyen [16], including viscoelasticity, but under continuous electrostatic loading, with the key finding that increased viscoelastic relaxation times led to a higher electric field needed to initiate the crack, with a subsequent decrease in crack propagation speed.

In contrast, our goal in the present work is to determine how viscoelasticity impacts crack initiation and propagation that results from a constant electrostatic (applied voltage) loading, analogous to an electromechanical creep test. The results from this study are shown in Fig. 6. In Fig. 6(*a*) we see that as the viscosity η, and thus the relaxation time τ_r, increases for the same applied voltage, a longer time is required for the crack to reach its maximum propagation distance Δy.

However, as shown in Fig. 6(*b*), if the time is normalized by the relaxation time τ_r, we find that the times for crack initiation all overlap. This leads to the conclusion, as previously observed for the electromechanical snap-through problem, that viscoelasticity again simply scales, in a linear proportion to the relaxation time, the amount of time it takes for an electrostatically nucleated crack to initiate, propagate, and travel its maximum distance.

4 Conclusion

In conclusion, we have used a nonlinear, dynamic viscoelastic finite element model to study electrostatically driven creeplike electromechanical instabilities in viscoelastic dielectric elastomers. We focused on two examples of electrostatically driven electromechanical instabilities that have been observed experimentally, i.e., the well-known snap-through instability, and the case of a cracklike defect that nucleates and propagates from a bursting drop in a dielectric elastomer. Our main finding is that when the relevant instability time is normalized by the viscoelastic relaxation time, that a universality in terms of the time needed to nucleate the instability is observed.

Acknowledgment

H.S.P. and J.W. acknowledge the support of the Mechanical Engineering Department at Boston University. T.D.N. acknowledges the support of the Mechanical Engineering Department at Johns Hopkins University.

References

[1] Carpi, F., Bauer, S., and Rossi, D. D., 2010, "Stretching Dielectric Elastomer Performance," Science, **330**, pp. 1759–1761.
[2] Brochu, P., and Pei, Q., 2010, "Advances in Dielectric Elastomers for Actuators and Artificial Muscles," Macromol. Rapid Commun., **31**, pp. 10–36.
[3] Biddiss, E., and Chau, T., 2008, "Dielectric Elastomers As Actuators for Upper Limb Prosthetics: Challenges and Opportunities," Med. Eng. Phys., **30**, pp. 403–418.
[4] Bar-Cohen, Y., 2005, "Biomimetics: Mimicking and Inspired-by Biology," Proc. SPIE, **5759**, pp. 1–8.
[5] Mirfakhrai, T., Madden, J. D. W., and Baughman, R. H., 2007, "Polymer Artificial Muscles," Mater. Today, **10**(4), pp. 30–38.
[6] O'Halloran, A., O'Malley, F., and McHugh, P., 2008, "A Review on Dielectric Elastomer Actuators, Technology, Applications, and Challenges," J. Appl. Phys., **104**, p. 071101.
[7] Zhang, X., Wissler, C. L. M., Jaehne, B., and Kovacs, G., 2005, "Dielectric Elastomers in Actuator Technology," Adv. Eng. Mater., **7**(5), pp. 361–367.
[8] Zhang, X. Q., Wissler, M., Jaehne, B., Broennimann, R., and Kovacs, G., 2004, "Effects of Crosslinking, Prestrain and Dielectric Filler on the Electromechanical Response of a New Silicone and Comparison With Acrylic Elastomer," Proc. SPIE, **5385**, pp. 78–86.
[9] Plante, J.-S., and Dubowsky, S., 2006, "Large-Scale Failure Modes of Dielectric Elastomer Actuators," Int. J. Solids Struct., **43**, pp. 7727–7751.
[10] Keplinger, C., Kaltenbrunner, M., Arnold, N., and Bauer, S., 2008, "Capacitive Extensometry for Transient Strain Analysis of Dielectric Elastomer Actuators," Appl. Phys. Lett., **92**, p. 192903.
[11] Hong, W., 2011, "Modeling Viscoelastic Dielectrics," J. Mech. Phys. Solids, **59**, pp. 637–650.
[12] Zhao, X., Koh, S. J. A., and Suo, Z., 2011, "Nonequilibrium Thermodynamics of Dielectric Elastomers," Int. J. Appl. Mech., **3**(2), pp. 203–217.
[13] Foo, C. C., Cai, S., Koh, S. J. A., Bauer, S., and Suo, Z., 2012, "Model of Dissipative Dielectric Elastomers," J. Appl. Phys., **111**, p. 034102.
[14] Wang, H., Lei, M., and Cai, S., 2013, "Viscoelastic Deformation of a Dielectric Elastomer Membrane Subject to Electromechanical Loads," J. Appl. Phys., **113**, p. 213508.
[15] Tagarielli, V. L., Hildick-Smith, R., and Huber, J. E., 2012, "Electro-Mechanical Properties and Electrostriction Response of a Rubbery Polymer for EAP Applications," Int. J. Solids Struct., **49**, pp. 3409–3415.
[16] Park, H. S., and Nguyen, T. D., 2013, "Viscoelastic Effects on Electromechanical Instabilities in Dielectric Elastomers," Soft Matter, **9**, pp. 1031–1042.
[17] Buschel, A., Klinkel, S., and Wagner, W., 2013, "Dielectric Elastomers—Numerical Modeling of Nonlinear Visco-Electroelasticity," Int. J. Numer. Methods Eng., **93**, pp. 834–856.
[18] Khan, K. A., Wafai, H., and Sayed, T. E., 2013, "A Variational Constitutive Framework for the Nonlinear Viscoelastic Response of a Dielectric Elastomer," Comput. Mech., **52**, pp. 345–360.
[19] Pelrine, R., Kornbluh, R., Pei, Q., and Joseph, J., 2000, "High-Speed Electrically Actuated Elastomers With Strain Greater Than 100%," Science, **287**, pp. 836–839.
[20] Wang, Q., Suo, Z., and Zhao, X., 2012, "Bursting Drops in Solid Dielectrics Caused by High Voltages," Nat. Commun., **3**, p. 1157.
[21] Zhao, X., Hong, W., and Suo, Z., 2007, "Electromechanical Hysteresis and Coexistent States in Dielectric Elastomers," Phys. Rev. B, **76**, p. 134113.
[22] Suo, Z., Zhao, X., and Greene, W. H., 2008, "A Nonlinear Field Theory of Deformable Dielectrics," J. Mech. Phys. Solids, **56**, pp. 467–486.
[23] Park, H. S., Suo, Z., Zhou, J., and Klein, P. A., 2012, "A Dynamic Finite Element Method for Inhomogeneous Deformation and Electromechanical Instability of Dielectric Elastomer Transducers," Int. J. Solids Struct., **49**, pp. 2187–2194.
[24] Park, H. S., Wang, Q., Zhao, X., and Klein, P. A., 2013, "Electromechanical Instability on Dielectric Polymer Surface: Modeling and Experiment," Comput. Methods Appl. Mech. Eng., **260**, pp. 40–49.
[25] Suo, Z., 2010, "Theory of Dielectric Elastomers," Acta Mech. Solida Sinica, **23**(6), pp. 549–578.
[26] Vu, D. K., Steinmann, P., and Possart, G., 2007, "Numerical Modelling of Non-Linear Electroelasticity," Int. J. Numer. Methods Eng., **70**, pp. 685–704.
[27] Zhao, X., and Suo, Z., 2007, "Method to Analyze Electromechanical Instability of Dielectric Elastomers," Appl. Phys. Lett., **91**, p. 061921.
[28] Arruda, E. M., and Boyce, M. C., 1993, "A Three-Dimensional Constitutive Model for the Large Stretch Behavior of Rubber Elastic Materials," J. Mech. Phys. Solids, **41**(2), pp. 389–412.
[29] Wissler, M., and Mazza, E., 2007, "Mechanical Behavior of an Acrylic Elastomer Used in Dielectric Elastomer Actuators," Sensors Actuators A, **134**, pp. 494–504.
[30] Reese, S., and Govindjee, S., 1998, "A Theory of Finite Viscoelasticity and Numerical Aspects," Int. J. Solids Struct., **35**(26–27), pp. 3455–3482.
[31] Hughes, T. J. R., 1987, *The Finite Element Method: Linear Static and Dynamic Finite Element Analysis*, Prentice-Hall, Englewood Cliffs, NJ.
[32] Simo, J. C., Taylor, R. L., and Pister, K. S., 1985, "Variational and Projection Methods for the Volume Constraint in Finite Deformation Elasto-Plasticity," Comput. Methods Appl. Mech. Eng., **51**, pp. 177–208.
[33] Nguyen, T. D. 2010, "A Comparison of a Nonlinear and Quasilinear Viscoelastic Anisotropic Model for Fibrous Tissues," Proceedings of the IUTAM Symposium on Cellular, Molecular and Tissue Mechanics, Woods Hole, MA, June 18–21, K. Garikipati and E. M. Arruda, eds., Springer, New York, Vol. 16, pp. 19–29.
[34] Tahoe, 2013, SourceForge.net, http://sourceforge.net/projects/tahoe/